37
12-17-77
Special Distr.

WAPD-TM-1313

DOE Research and Development Report

The Susceptibility of Unirradiated Recrystallized Zircaloy-4 Tubing to Stress Corrosion Cracking

(LWBR Development Program)

N. W. Polan and R. P. Tucker

Bettis Atomic Power Laboratory
West Mifflin, Pennsylvania 15122

080 6000

December 1977

Prepared for the
U.S. Department of Energy
By Westinghouse Electric Corporation
Under Contract No. EY-76-C-11-0014

DISCLAIMER

THE SUSCEPTIBILITY OF UNIRRADIATED RECRYSTALLIZED ZIRCALOY-4 TUBING TO STRESS CORROSION CRACKING

(LWBR Development Program)

N. W. Polan and R. P. Tucker

December 1977

Contract No. EY-76-C-11-0014

Printed in the United States of America
Available from
National Technical Information Service
U. S. Department of Commerce
5285 Port Royal Road
Springfield, VA 22161

NOTE

This document is an interim memorandum prepared primarily for internal reference and does not represent a final expression of the opinion of Westinghouse. When this memorandum is distributed externally, it is with the express understanding that Westinghouse makes no representation as to completeness, accuracy, or usability of information contained therein.

BETTIS ATOMIC POWER LABORATORY PITTSBURGH, PENNSYLVANIA

Operated for the U. S. Department of Energy By
WESTINGHOUSE ELECTRIC CORPORATION

TABLE OF CONTENTS

LIST OF TABLES

LIST OF FIGURES

THE SUSCEPTIBILITY OF UNIRRADIATED RECRYSTALLIZED ZIRCALOY-4 TUBING TO STRESS CORROSION CRACKING (LWBR Development Program)

ABSTRACT

Stress corrosion cracking (SCC) in unirradiated recrystallized Zircaloy-4 internally pressurized tubing specimens in atmospheres containing iodine vapor, cesium, or combinations of iodine and cesium is evaluated experimentally in terms of the effects of internal surface flaw morphology, iodine and cesium concentrations, tubing hydrogen content, test temperature, and test atmosphere water vapor content on the time to failure. The iodine vapor SCC data are analyzed in the framework of a fracture mechanics model. Expressions are developed which relate the iodine SCC threshold stress and lifetime for stresses above threshold to temperature, iodine concentration, and surface flaw geometry.

THE SUSCEPTIBILITY OF UNIRRADIATED RECRYSTALLIZED ZIRCALOY-4 TUBING TO STRESS CORROSION CRACKING (LWBR Development Program)

N. W. Polan and R. P. Tucker

I. INTRODUCTION

In recent years, evaluation of the performance of water reactor fuel rods has provided evidence that fission product stress corrosion cracking (SCC) is a likely cause of a number of low ductility failures which have occurred in Zircaloy cladding, especially under power ramping conditions. These observations have stimulated active test programs throughout much of the industry to characterize the behavior of Zircaloy in potential stress corrosion environments. At Bettis the program focus has been to develop a SCC criterion for establishing stress and operational limits for the Light Water Breeder Reactor (LWBR). Previous experimental and analytical studies have assessed the susceptibility of stress relieved (SRA) and, to a lesser extent, recrystallized (RXA) Zircaloy-4 tubing to halogen stress corrosion cracking (References 1-4). This report extends the evaluation of unirradiated recrystallized Zircaloy-4 tubing in regard to its susceptibility to iodine and cesium SCC.

The analytical basis for the Bettis SCC criterion is the linear elastic fracture mechanics model of Kreyns et al., (Reference 3), which predicts failure time as a function of stress, temperature, and tubing surface flaw morphology. Specifically, the time to failure due to iodine stress corrosion in internally pressurized SRA Zircaloy-4 tubing specimens was given by Equation (1), (References 3, 4):

$$t_f = \frac{I_2^{-3/4} \exp \frac{Q}{RT}}{C_o \sigma_\theta^4 Y^4} \left[\frac{1}{a_o} - \frac{1}{a_c} \right] , \qquad (1)$$

where t_f = time to failure (minutes)
σ_θ = applied hoop stress (psi)
a_o = initial internal surface flaw depth (inches)
a_c = critical flaw depth (inches) to cause instantaneous failure by stress rupture ($a_c/w = 1 - \sigma_\theta/\sigma_{ult}$), w = wall thickness
σ_{ult} = pressure burst hoop stress (psi)
Y = fracture mechanics flaw geometry factor
C_o = material constant
R = gas, constant (1.987 cal/°K-mole)
Q = activation energy (cal/mole)
T = temperature (°K)
I_2 = iodine concentration (mg/dm^2).

Furthermore, an analytical expression for the threshold hoop stress ($\sigma_{\theta th}$), the stress below which iodine SCC will not occur, was developed and experimentally verified for SRA tubing specimens in Reference 4. This expression is

$$\sigma_{\theta_{th}} = \frac{K_{ISCC}}{\sqrt{a_o}\, Y} = \frac{2710-3T}{\sqrt{a_o}\, Y}\, I_2^{-3/16} \qquad (2)$$

It is to be noted that the threshold hoop stress, which is directly proportional to the minimum stress intensity required for iodine SCC (K_{ISCC}), is expressed in Equation 2 as a direct function of the iodine surface concentration (mg/dm^2) and the test temperature in degrees Fahrenheit and as an inverse function of the tubing surface flaw morphology.

The present report characterizes the stress corrosion propensity of unirradiated Zircaloy-4 RXA tubing under a variety of conditions and evaluates the constants in Equations (1) and (2) for iodine SCC in RXA tubing. The following areas are addressed: (1) examination of the time-to-failure correlation and evaluation of the threshold prediction expression for RXA tubing, (2) determination, in a limited study, of the effects of tubing hydrogen content on iodine SCC, (3) determination of the iodine SCC response of RXA tubing under fixed-strain loading conditions, (4) examination of the effects of water vapor on SCC in internally pressurized RXA tubing, and (5) determination of the susceptibility of internally pressurized RXA tubing to cesium SCC.

The hydrided tubing tests were undertaken to investigate the reported improved resistance of hydrided Zircaloy to iodine SCC. It was suggested in Reference 5 that hydrogen in stressed split-ring iodine SCC tests migrated to the regions of higher tensile stresses present at SCC crack tips and thereby reduced the stress level at the crack tips, thus arresting or slowing crack propagation. Furthermore, it was suggested that slight stress-induced rotations of pre-existing hydrides in heavily hydrided Zircaloy could blunt cracks.

In Reference 5 it was also indicated that water vapor deliberately added to the test environment inhibited iodine SCC in cold-drawn Zircaloy stressed split ring tests. The present study tests were designed to investigate this phenomenon and to evaluate previous Bettis iodine SCC tests which contained one atmosphere of nominal 70% relative humidity air.

Cesium, a highly reactive fission product, is produced in relative abundance in fuel rods and is found at rod cladding surfaces (Reference 6). It has been shown to cause liquid metal embrittlement of Zircaloy under dynamic deformation conditions (References 7-11). Results are reported here on a limited number of tests on Zircaloy tubing with cesium alone or in combination with iodine.

Although not a subject of the present study, it should be noted that recently solid cadmium at 300°C, liquid cadmium at 340°C and cesium saturated with cadmium at 300°C have been shown to embrittle Zircaloy (Reference 12). Cadmium, a fission product of UO_2 fuel, which occurs at a significantly lower yield than either iodine or cesium (Reference 13) is thus another potential corrodant that could lead to cladding failure.

II. MATERIALS DESCRIPTION

Specimens for these tests were fabricated from RXA Zircaloy-4 tubing which was manufactured according to the following schedule:

76.9% cold tube reduction
1300°F vacuum anneal for 3-4 hours
67.3% cold tube reduction
1300°F vacuum anneal for 3-4 hours
68.1% cold tube reduction
1225°F vacuum anneal for 5-6 hours

The nominal as-received tubing dimensions were 0.3105 ± 0.002 in. O.D. x 0.262 ± 0.001 in.I.D. with a minimum wall thickness of 0.0225 in. Vendor-certified mechanical properties for the lots of tubing used in these tests appear in Table Ia. and Ib. Pressure burst test data obtained in this study on the various tubing lots appear in Table Ic. Specimens taken from a particular lot will be hereafter identified by the letter prefix indicated in Table Ia.

American Chemical Society certified resublimed iodine and Fisher electrolytic cesium were the corrosive agents used. The iodine contained ≤ 0.005% Cl + Br and ≤ 0.008% nonvolatiles as impurities. The gas used to internally pressurize specimens was 99.995% pure argon. Analyzed impurities in the Ar were: O < 5 ppm, N < 10 ppm, H < 5 ppm, H_2O ≤ 1 ppm, and carbon-bearing gases < 5 ppm.

III. EXPERIMENTAL PROCEDURE

The specimens used for the majority of these tests were capped tubes that were internally pressurized at room temperature with argon gas to provide a biaxial stress. The hoop stress experienced by the cladding was calculated employing the standard relationship for thin-walled tubing with the internal pressure corrected for the nonideal behavior of argon. Specimens were five inches long with a nominal four-inch long gage length which was obtained by chemically etching the tubing O.D. Nominal wall thickness in the gage section was 0.012 in. Individual specimens were measured internally with an air gauge. External dimensions were obtained using a vernier micrometer and a Pratt and Whitney bench micrometer with wedge anvils which limited the load applied to the specimen to 4 oz. The iodine was weighed and sealed in quartz capillaries which were inserted into the specimen and broken immediately prior to pressurizing with argon gas and seal welding. Failure of the specimens was determined by weight loss due to the loss of argon. Specimens that exhibited nonuniform deformation during testing or whose failure time differed significantly from similarly tested specimens were examined metallographically in transverse cross-section at the failure site in order to measure wall thickness eccentricity.

The low water vapor specimens and cesium specimens were fabricated in the same manner as the other internally pressurized specimens but were charged with the corroding species and pressurized under conditions controlled to eliminate moisture in the specimen cavity. To accomplish this, open-ended specimens and open quartz capillaries to be used to transfer the I_2 and Cs for weighing and specimen insertion were placed in quartz bulbs evacuated to 10^{-5} torr and heated in a dynamic vacuum to 150°C for 4 hours. The bulbs were then sealed and transferred to a glove box purged with flowing argon. Specimens and capillaries were then removed from the sealed bulbs and were charged with iodine and/or cesium which was weighed out from fresh sealed containers in the glove box. Specimens were pressurized with argon gas and valved in the glove box. They were then immediately removed from the glove box and resistance welded between the valve and specimen cavity. The resultant H_2O and O_2 concentrations in a typical specimen to be pressurized to 40,000 psi at 680°F are ~ 0.03 ppm H_2O + .1 ppm O_2 compared with ~ 2 ppm H_2O + 26 ppm O_2 for a conventionally prepared specimen containing one atmosphere of 70% relative humidity air. (These concentrations are calculated as parts per million by weight with respect to the tube being loaded with thoria-urania sintered fuel pellets.)

For the hydrided tubing tests, hydrogen was added to the tubing by gas equilibration with zirconium hydride powder at 1225°F for 4 hours. Levels of ~ 50 and ~ 180 ppm were proposed so that hydrogen would be present both in solid solution and as the hydride precipitate. The solid solubility at the two test temperatures of 680 and 600°F is ~ 135 and ~ 85 ppm, respectively. The 600°F temperature was chosen to provide a higher ratio of precipitated to dissolved hydrogen.

In the strain-limited tests, the specimens were loaded by means of the differential thermal expansion of internal stainless steel mandrels. Open tubing specimens were dimensioned and DPH fiducial reference marks were placed along the length of the tubing specimens in order to monitor axial strains. The mandrels were chilled to - 321°F and the tubes preheated to 550°F in order to facilitate mandrel insertion and to form an initial interference fit and maximize the obtainable strain at test temperature. Specimens were then end-cap welded, charged with iodine, pressurized with argon to 50 psi, and

sealed. They were then encapsulated individually in evacuated quartz bulbs in order to preserve good surface finish for post-test dimensioning and to permit rapid testing for argon leakage from the specimen by ionization of the bulb atmosphere. The mandrels contained fifteen 0.020 inch wide longitudinal grooves equally spaced around the circumference. This exposed to the iodine vapor the tubing surface spanning the grooves directly, which is approximately one third of the total tubing surface. (Stated surface concentrations for the mandrel specimens refer to this exposed area.) The tests, with the exception of the 2000 hour tests reported below, were single cycles with no intermediate cooling in order to maintain the maximum axial elastic strain and prevent shifting of the mandrels. Iodine levels of 4 and 50 mg/dm^2 were used. Internally pressurized specimens from the same lengths of tubing were also tested at 4 mg/dm^2 I_2 in order to establish constant-stress test behavior for the same material. Most mandrel tests were conducted at 680°F. Two specimens at 50 mg/dm^2 I_2 were tested at 600°F where stress relaxation was less than at 680°F. After testing, transverse cross-sections of the specimens were metallographically examined for partial cracks. These sections were taken at the location of maximum biaxial stress which was over the center of the mandrel. To obtain, as a function of time, an estimate of the degree of stress relaxation caused by conversion of elastic to plastic strain, a separate series of open-ended tubing lengths was prepared with mandrels and placed in test at 680°F for periods of 1, 4, 16, 72, 300 and 1000 hours.

Scanning electron microscope specimens were cut from the same lengths of tubing between the SCC specimens at intervals down the 10-foot length of each tube in order to characterize the shapes of the initial internal surface flaws. Specimens for transverse metallography were also taken at the same locations in order to estimate the maximum I.D. surface flaw depths.

IV. RESULTS AND CONCLUSIONS

A. Tubing Internal Surface Flaw Characterization

Two types of internal surface flaws have been observed in previous studies of Zircaloy tubing (Reference 2). RXA tubing contained predominantly "grooves" (elongated flaws), SRA tubing principally contained small pits or dimples (~ equiaxed). In the ensuing fracture mechanics model (Reference 3),

differences in failure behavior were adequately described by assigning shape factors, Y, of 2.0 and 1.286 to grooves and pits, respectively.

The internal surface flaw geometry for each tubing length used in this study was examined in the scanning electron microscope. Observations are summarized in Table II along with transverse cross-section measurements of the maximum flaw depth and the average of the ten greatest flaw depths observed for each tube. The overall appearance of the various tube surfaces differed significantly in the ratio of pits to grooves; however, some elongated flaws were observed in all specimens, either as clearly defined grooves or a series of elongated or interconnected aligned pits. In addition, all microscopy specimens contained at least one sharply defined longitudinal scratch. The depths of these latter flaws varied but were comparable to, or smaller than, the accompanying pits and grooves.

Since all specimens contained some groove-like flaws of aspect ratio $\frac{a}{2c} \leq 0.1$ (a = flaw depth, 2c = flaw length) and grooves are the more severe flaws from a fracture mechanics standpoint, all tested tubing lots were initially characterized by taking Y = 2, the fracture mechanics correction factor corresponding to $\frac{a}{2c} = 0.1$. As will be shown, this assignment, Y = 2, adequately represents the failure data.

An accurate representation of the flaw depths is more difficult. The actual SCC specimen cannot be examined before testing to determine the location of the most severe flaw, nor can it be accurately measured after failure. Abnormally large flaws may exist undetected in a specimen gage section and cause premature failure inconsistent with the failure time calculated using an assumed flaw size and Equation (1). For example, above threshold, a flaw 25% deeper than expected will reduce the failure time by approximately 20% for a specimen tested at $\sigma/\sigma_{ult} = 0.5$. Similarly, measurements of wall thickness eccentricity cannot be made before test, and sufficiently accurate measurements cannot be obtained from badly bowed or non-uniformly bulged specimens after test. These two effects are principally responsible for the scatter in the data discussed below.

B. Effects of Iodine SCC in Internally Pressurized Tubing

In order to evaluate the constants in Equation (1) and to determine the iodine sensitivity of RXA tubing, internally pressurized tubing specimens

were tested at iodine surface concentrations of 0, 0.1, 0.5, and 4 mg/dm^2; nominal hoop stresses of 22, 25, 30, 35, and 40 ksi; and temperatures of 680, 720, and 750°F. Detailed test conditions and failure data appear in Table III. Test times are given for those specimens which did not fail. The fourth column of the table lists the nominal hoop stress at the actual failure location. For straight, uniformly deformed specimens this stress is calculated using the pretest I.D. and O.D. measurements which were made at $\frac{1}{2}$-inch intervals along the length of the tube and at the slight etching undercuts at the ends of the gage lengths. For moderately bowed specimens which were not bulged, wall thickness data from transverse metallographic sections at the failure site were used -- in some of the slightly bowed specimens, no wall thickness eccentricity could be measured. Sufficiently accurate data on pretest wall thickness eccentricity could not be obtained after test for the badly bowed or bulged specimens. The wall thickness eccentricity observed in specimens from tubes B, C, D, E and F was caused by nonuniform thinning during gage section etching. This deficiency was corrected before preparing the G, H, J, K, L and M series specimens. All data in Table III are plotted in Figure 1. Each part of Figure 1 presents the time-to-failure results at various stresses for specimens from a given length of tubing at specified iodine concentrations. The tubing lengths and corresponding symbols are identified at the left margin of each part of the figure. As noted in the figure caption, the fully shaded symbols are for 4 mg/dm^2 I_2, the symbols shaded in the upper half are for 0.5 mg/dm^2 I_2, the symbols shaded in the lower half are for 0.1 mg/dm^2 I_2, and the open symbols are for control specimens without iodine where failure is predominantly by stress rupture. Curves based on Equations (5) and (7) developed below are shown in Figure 1 for iodine concentrations of 0.5 mg/dm^2 I_2 (upper curve) and 4 mg/dm^2 I_2 (lower curve). Note that the curves display three regimes of behavior: (1) at high stress in the vicinity of the 0.2% yield stress the failure is predominantly by stress rupture, (2) at intermediate stresses the slope of the failure curve increases reflecting the deleterious effect of iodine, and (3) at lower stresses a threshold dependent on iodine concentration is reached below which iodine SCC does not occur and again failure is predominantly by stress rupture at very long times.

In evaluating the effect of iodine concentration on failure time in the stress dependent portion of the curves (i.e., above threshold) use was made of Equation (1) in an attempt to normalize the data with respect to all the variables except iodine concentration. For this purpose, the iodine concentration was omitted and the material constant C_o in Equation (1) was redefined as:

$$C_o = \frac{\exp\,(42{,}900/RT)}{t_f\,\sigma_\theta^4\,Y^4}\left[\frac{1}{a_o} - \frac{1}{a_c}\right], \qquad (3)$$

with dimensions of $(psi^4 \cdot in. \cdot min)^{-1}$ where

Q = 42,900 cal/mole as determined in Reference 3 for RXA tubing
t_f = failure time, minutes
σ_θ = applied hoop stress, psi
a_o = initial flaw depth, inch
a_c = critical flaw depth, inch

Figure 2 is a plot of the Equation (3) constant C_o as a function of iodine concentration for all the relatively uniform specimens of Table III (i.e., those which were not significantly bowed or bulged at failure). Data were not used from deformed specimens and from those tubing lengths where valid data exist at only a single iodine concentration. Values for a_o were taken to be the average maximum values of Table II for the respective tubing lengths. The broken lines in Figure 2 are the least squares linear regressions for the individual tubing lots. The slope, m, of each curve is indicated. The solid line is the least squares fit for all the data and yields:

$$C_o = 2.6 \times 10^{-5}\, I_2^{.781} \quad . \qquad (4)$$

The relative displacements of the curves for each tubing length is probably indicative of the sensitivity of C_o to measurement errors in assigning the flaw geometry factor, $Y^4 a_o$, to each length since Equation (3) should normalize C_o for these effects. Tubes F and H, the extremes of the Figure 2 distribution,

are from the same lot of tubing -- the observed separation of data is apparently not solely due to lot-to-lot variability. The most likely cause of this data separation is the inability to adequately characterize the appropriate $\overline{a}_o$ for each tubing length (e.g., B, C, D, etc.). Subtle flaw morphologies peculiar to an individual tubing length and unidentifiable by current SEM and metallographic procedures may also contribute to this variation. The effect of surface inclusions or precipitates may be significant, as suggested in Reference 11e, where observations of second phase silicon-rich particles were observed at crack initiation sites. An inaccuracy in the flaw characterization, however, does not affect the slope of the curve for a given tubing length and the data show that for iodine concentrations up to 4 mg/dm^2, the sensitivity of failure time above threshold to iodine concentration in RXA Zircaloy-4 tubing generally agrees with SRA tubing where the exponent on iodine concentration was estimated to be 3/4 (Reference 4).

Equation (1) may now be written for RXA Zircaloy-4 tubing as

$$t_f = \frac{I_2^{-.781} \exp\left(\frac{42,900}{RT}\right)}{1.56 \times 10^{-3} \sigma_\theta^4 Y^4} \left[\frac{1}{a_o} - \frac{1}{a_c}\right] , \qquad (5)$$

where the time to failure, t_f, is given in hours. Representative plots of Equation (5) appear in each part of Figure 1 for the various tubing lots, taking Y = 2.0 and a typical flaw depth of 0.00025 in. Equation (5), using these values for Y and a_o, thus yields agreement with all valid I_2 SCC failures observed in this study.

C. Effects of Iodine Concentration and Temperature on K_{ISCC}

An additional group of internally pressurized specimens was tested at stresses near the threshold for 720°F and 0.1 mg/dm^2 in order to examine lot-to-lot variability and to increase the data base for SCC failures at low iodine levels -- many of the low iodine specimens in Table III were bowed and bulged.

The test conditions and failure data for these specimens appear in Table IV. Many specimens have not failed. The stresses were calculated as in Table III and the data are plotted in Figure 3. Control specimens at 720°F

(Table III) containing no iodine are indicated by "X" and the broken line in Figure 3. For RXA tubing at 720°F and 0.1 mg/dm^2 iodine, failure appearances and times indicate that stress rupture plays an important role in the failure of many of these specimens over the entire stress range examined. In fact, comparison of the data at an iodine concentration of 0.1 mg/dm^2 with the control specimen failure data in Figure 1 suggest that over the temperature range from 680°F to 750°F stress rupture is likely dominant in the failure of many of these specimens.

In order to develop an analytical expression for the threshold hoop stress as a function of temperature, iodine concentration and flaw geometry, we proceed as in Reference 4 and assume that the minimum stress corrosion crack velocity, v^*, as the stress intensity factor K_I approaches K_{ISCC}, is invariant with respect to iodine concentration. This requires that $v^* = C\,K^4_{ISCC}$ (where $C = C_o I_2^{.781}$). Thus, $K_{ISCC} = \frac{v^{*\frac{1}{4}}}{c}$ or

$$K_{ISCC} = K_o (I_2)^{(-.781)/4}, \qquad (6)$$

where K_o represents the temperature dependence and is obtained by substitution of known values for K_{ISCC} at known iodine concentrations and different temperatures (Reference 3). From Figure 1 we can estimate threshold stresses for tubes J and D at 4 mg/dm^2 I_2 and 680 and 750°F respectively; Reference 2 yields similar data on an earlier lot of RXA tubing. These data are presented in Table V.

Now $\sigma_{\theta th} = \frac{K_{ISCC}}{\sqrt{a_o}\,Y}$, by definition, and the J and D data points of Table V yield

$$\sigma_{\theta_{th}} = \frac{(1572.8 - 1.059\,T)\,I_2^{-.19525}}{\sqrt{a_o}\,Y}, \qquad (7)$$

where T is in °F. In determining the numerical constants in Equation (7), a_o was taken to be 0.0002 inch consistent with the measured average maximum values in Table II for J and D specimens and the actual measured value for an earlier lot of RXA tubing.

Calculation of the threshold stress using Equation (7) is very sensitive to the a_o value. The measured a_o values are subject to substantial

uncertainty. Thus, representative threshold stresses have been calculated employing Equation (7) and a nominal a_o = 0.00025 inch. These threshold stresses appear in Table VI and as the threshold portion of the curves in Figure 1. All near-threshold valid SCC failures observed in this study for 4 and 0.5 mg/dm^2 I_2 are lower bounded by Equation (7) with Y = 2 and a_o equal to a nominal 0.00025 in. Equation (7) and the results appearing in Table VI support the statement that the 0.1 mg/dm^2 I_2 specimen failures are complicated by stress rupture.

In retrospect, the inclusion of the 0.1 mg/dm^2 I_2 data in the calculation of the iodine sensitivity parameters in Figure 2 is justified on the following basis: (1) these 0.1 mg/dm^2 I_2 data, to the extent that they are influenced by stress rupture, provide conservative estimates of C_o, (2) curves for tubing lengths B and H, plotted in Figure 2, span all the 0.1 mg/dm^2 I_2 data but are not themselves based on any 0.1 mg/dm^2 I_2 data, (3) deleting the 0.1 mg/dm^2 I_2 data and the two anomalous 0.5 mg/dm^2 I_2 data points from tube F, yield the same I_2 exponent (-.781) as in Equation (5) and a slightly lower numerical constant, 1.44×10^{-3} rather than 1.56×10^{-3}.

D. Effects of Water Vapor on Iodine SCC in RXA Zircaloy-4 Tubing

Tests to determine the effects of water vapor on iodine stress corrosion cracking were conducted under the conditions specified in Table VII. These failure data appear in Figure 4 along with the nominal 4 mg/dm^2 I_2 curves calculated using Equations (5) and (7). Critical failed specimens were sectioned, metallographically mounted and polished for measurement of wall thickness variations in order to refine the stress calculations.

The difference in failure times between specimens M16 and M12 might be taken to imply longer survival at lower H_2O levels. However, the actual stresses at the failure locations for these two specimens are near threshold, and such a variation in failure between identically prepared specimens has been observed in previously reported data near threshold, e.g., Reference 3. A comparison of specimen M19 and M18 failure times also is not valid because specimen M18 failed outside the gage length and was found to contain anomalous internal contamination and apparent iodine reaction products at the thick-walled failure site.

Figure 4 shows that the low water vapor specimen failure times are consistent with the failure curves predicted for 4 mg/dm^2 I_2 using Equations (5) and (7), which were based on data for specimens at a nominal water vapor concentration. In this limited investigation no water vapor dependence of iodine SCC has been identified for the iodine and water vapor concentrations investigated.

E. Effects of Tubing Hydrogen Content on Iodine SCC in Internally Pressurized RXA Zircaloy-4 Tubing

As described in the introduction, interest has been expressed in the possibility of dissolved hydrogen migrating to high stress regions at potential SCC crack tips and reducing the tensile stresses there, consequently arresting or slowing crack growth. Stress-induced reorientation of hydride platelets may have a similar effect. A limited number of tests were conducted on hydrided tubing specimens under the conditions specified in Table VIII. All specimens that failed were sectioned, metallographically mounted and polished for measurement of wall thickness variations in order to refine the stress calculations. Failure data are represented graphically in Figure 5.

The data are in reasonable agreement with the nominal 4 mg/dm^2 I_2 curves, which were calculated using Equations (5) and (7) for as-received tubing of nominal hydrogen content. No marked effects of hydrogen concentrations up to 190 ppm can be identified at the test temperatures of 600 and 680°F -- all failures are lower bounded by the Y = 2, a_o = 0.00025 in. curves. While no strong conclusion can be drawn, comparison of these failure data in Table VIII for specimens all from a given length of tubing suggest that there may be a slightly increased susceptibility to iodine SCC in deliberately hydrided specimens at stresses above threshold, at least under these fixed-stress conditions.

F. Stress Corrosion Effects of Cesium in Internally Pressurized RXA Zircaloy-4 Tubing

The effects of cesium on SCC in internally pressurized RXA Zircaloy-4 tubing have been investigated under the conditions presented in Table IX. Iodine SCC control specimen data from the same tubing length, M, appear in

Table VII. The cesium concentration of 28 mg/dm^2 was established based on fission yield to represent an equivalent state of 4 mg/dm^2 I_2. The high cesium concentration specimens (800, 3200 mg/dm^2) were tested to examine liquid metal embrittlement (LME) effects. Specimens were tested at 392°F because of a report that temperatures less than 480°F were required* to cause failures of Zircaloy tubing in cesium (Reference 9).

Only one specimen in the cesium test series has failed, and that single failure was caused by stress rupture at an etching undercut at the end of the gage section of the specimen. The specimens with 28 mg/dm^2 cesium have survived > 25 times longer than specimens containing 4 mg/dm^2 I_2 under otherwise identical conditions. The Cs + I_2 specimens have survived > 15 times longer than specimens containing 4 mg/dm^2 I_2 alone. In these internally pressurized quasi-static** stress corrosion tests under the conditions tabulated, the effects of cesium alone or in combination with its fission yield equivalent iodine concentration are much less severe than those observed for iodine alone, at 680°F.

The cesium-induced failures cited in the literature (References 7-11) were all obtained under dynamic conditions at high stress intensities in liquid cesium with low oxygen content. Presumably the protective oxide layer on the Zircaloy must be broken and prevented from reforming in order to permit liquid metal embrittlement by the cesium. Stanford Research Institute (SRI) data (Reference 11d) indicate, however, that the onset of cracking at 40°C occurs at less than 1% plastic strain, which SRI indicates as being of the same order as the strain involved in pellet-clad interaction cladding failures. Recent SRI results (Reference 11c) also indicate that presence of a small concentration of iron is necessary to cause LME and suggest that a localized Zr-Fe reaction occurs -- the reaction product being only sparingly soluble in cesium, LME is obtained only over a narrow iron concentration range.

---

* Subsequent failures have been observed at 572°F (Reference 11).

** Specimens are cooled to room temperature for weighing at least every 72 hours. Hoop stresses are consequently cycled by a factor of about 2.5 throughout the duration of the test.

The cesium tests reported here were conducted at low oxygen levels which caused failures in the other investigations, however, they were "quasi-static" -- the most highly stressed specimen went from 14 to 35 ksi during heating from room temperature to the test temperature, 750°F (35 ksi in this tubing corresponds to $K_I \sim 1$ ksi $\sqrt{in}$. assuming a 0.2 mil flaw depth which is quite a low stress intensity). No intentional iron contamination was introduced into these specimens. The survival of the Cs + I_2 specimens is probably due to the formation of stable CsI. The extent of applicability of equilibrium thermodynamics to compound formation in a strong irradiation field is not known. Thus, it is uncertain the extent to which cesium iodide will form in an operating fuel rod. Both cesium and iodine have been found on cladding inner surfaces (References 15 and 16). It has been proposed that cesium iodide can be decomposed by gamma-radiolysis (Reference 11a). Furthermore, fission products are released at different rates and migrate in such a way that nonuniform distributions are observed (e.g., References 14-16). Although a discussion of fuel rod chemistry is beyond the scope of this report, the point must be made that the current test results do not imply that iodine is not an active SCC agent in-pile solely because there is enough cesium present to form CsI.

G. Internal Mandrel Strain-Controlled Iodine SCC Tests

Internal mandrel iodine SCC tests on 0.576 in. O.D. SRA Zircaloy-4 tubing were conducted in order to compare cracking susceptibility under fixed-strain conditions, where the stress relaxes, to that observed in fixed-stress internally pressurized tube tests, since this condition is more representative of pellet-cladding behavior in an operating fuel rod than is a pressurized tube specimen. Total strains on the order of .4% were achieved through differential thermal expansion of stainless steel mandrels. Despite very high initial stresses that were developed in the mandrel tests (estimated over 46,000 psi hoop), there was no indication of cracking in these tests which were conducted at an iodine concentration of 4 mg/dm^2 and temperatures of 680 and 750°F. Indications from dimensional measurements were that the stresses relaxed rapidly to less than half the initial values thereby placing the stress level below threshold (K_{ISCC}) at 4 mg/dm^2 of iodine. It was not possible, therefore, to determine how accurately SCC failure in a decreasing

stress mode can be predicted by utilizing constant stress (pressurized tube) test data and a linear damage model.* Applying the linear damage rule to the estimated stress history of the test specimens did predict that cracking was unlikely, consistent with the test results. Experience with these tests showed that truly detailed comparison with pressurized tube data is difficult since the stresses must be estimated from measurement of small strains at temperature under biaxial loading. The same difficulty exists in an operating fuel rod.

A procedure utilizing high temperature bonded strain gages in a bridge network containing an empty tube to cancel thermal expansion strains was successful in providing an accurate measure of the total circumferential (e_θ) and axial (e_z) strains on heating to the test temperature. An estimate of the initial (loading) biaxial stresses can be obtained from pressure-burst data and corrections for the change in biaxial stress ratio through R and P anisotropy parameters. The principal difficulty comes thereafter in deducing the degree of stress relaxation by measurements of axial and diametral plastic strains on cooling to room temperature periodically during the course of the test. While the total strain remains constant, the stress depends on the residual elastic strains, computed as $\varepsilon_{Total} - \varepsilon_{Plastic}$. For the small diameter RXA tubing, this means that the computed stress will vary by about 4,000 psi for a permanent diametral change of 0.0001 inch. Measurement uncertainties at least this large are unavoidable. Therefore, the tests reported below were aimed primarily at determining whether stress corrosion cracking does or does not occur at long times at a given total strain.

RXA specimen test parameters appear in Table X. Companion constant-stress internally pressurized control specimens appear in Table III.e,g,h. Data from the series of open-ended mandrel specimens (intended to characterize the degree of stress relaxation) were erratic, due to the small diameter of the tubing and the inability to accurately measure the small dimensional changes after testing.

---

* Failure in the strain-limited tests was predicted when $\sum_i \frac{\Delta t_i}{(t_F)} = 1$ where Δt_i is the time spent at a nominal stress, σ_i; and $(t_F)_i$ is the time to failure in a test at constant stress, σ_i.

No thru-failures occurred in any of the internal mandrel RXA SCC specimens. This was confirmed by (1) ionization tests on the evacuated bulbs containing the specimens and (2) helium leak tests on the individual specimens. Furthermore, metallographic examination of transverse cross-sections of all specimens revealed no partial cracking occurred at the location of maximum biaxial stress, which is over the center of the mandrel. Stress corrosion was not induced during single cycle loading under any of the conditions tested.

V. SUMMARY

Analyses of stress corrosion test results on unirradiated RXA Zircaloy-4 tubing yield the following observations and conclusions:

1. The time to failure by iodine SCC at stresses above threshold, temperatures in the range of 680 to 750°F, and iodine concentrations of 0.5 to 4 mg/dm^2 can be bounded by:

$$t_F = \frac{I_2^{-.781} \exp(42{,}900/RT)}{1.56 \times 10^{-3} \sigma_\theta^4 Y^4} \left[\frac{1}{a_o} - \frac{1}{a_c} \right] ,$$

for unirradiated RXA Zircaloy-4 tubing. This equation gives a good lower bound fit to all valid SCC failures observed in this study, using Y = 2 and a_o = 0.00025 in. Data at 0.1 mg/dm^2 I_2 are scattered due to the influence of stress rupture.

2. The threshold stress for iodine SCC is given by

$$\sigma_{\theta_{th}} = \frac{(1572.8 - 1.059T) I_2^{-.19525}}{\sqrt{a_o} Y}$$

for unirradiated RXA Zircaloy-4 tubing at iodine concentrations of 0.5 and 4 mg/dm^2. All near-threshold valid SCC failures observed in this study at 4 and 0.5 mg/dm^2 I_2 are conservatively bounded by the above equation with Y = 2 and a_o equal to a nominal 0.00025 inch. Specimens at 0.1 mg/dm^2 I_2 fail at lower stresses by stress rupture.

3. No internally pressurized iodine SCC unirradiated RXA specimens have failed in less than 1460 hours at hoop stresses $\leq$ 30 ksi, temperatures of 680 and 720°F and iodine concentrations of 0.1 mg/dm^2.

4. No water vapor concentration dependence of iodine SCC has been identified at 680 and 750°F and iodine concentrations of 4 mg/dm^2 over the range of 0.03 ppm H_2O (+ .1 ppm O_2) to 2 ppm H_2O + (26 ppm O_2) (ppm by weight with respect to the specimen being loaded with binary fuel).

5. No marked effect of tubing hydrogen concentrations up to 190 ppm has been identified at test temperatures of 600 and 680°F at iodine concentrations of 4 mg/dm^2. While there is considerable scatter in the data, there seems to be a slight increased susceptibility to iodine SCC in the deliberately hydrided specimens for stresses above threshold.

6. In internally pressurized quasi-static SCC tests at cesium concentrations of 28 mg/dm^2, a test temperature of 680°F and hoop stress of 35 ksi, the effects of cesium alone or in combination with its fission yield equivalent iodine concentration are much less severe than those observed for iodine alone, under the same conditions. The Cs + I_2 specimens have survived > 15 times longer than corresponding I_2 specimens.

7. No thru-failures or partial cracks at the location of maximum biaxial stress occurred in any of the internal mandrel strain-limited SCC tests at 680°F, iodine concentrations up to 50 mg/dm^2, initially applied strains of 0.34% and test times up to 2015 hours.

ACKNOWLEDMENT

The authors gratefully acknowledge the assistance of K. B. Marsh, who carefully performed the bulk of the specimen preparation, dimensioning, and test monitoring; P. H. Kreyns, G. L. Spahr, and J. E. McCauley who proposed the analytical model applied to the data in this report; C. C. Busby who assisted in performing the pressure burst tests of Table I.c; and J. J. Kearns who assisted with the mandrel tests and provided helpful comments on the report.

REFERENCES

1. J. G. Weinberg, "Iodine Stress Corrosion Cracking of Zircaloy-4 Tubing", WAPD-TM-1048, February, 1974.

2. C. C. Busby, R. P. Tucker and J. E. McCauley, "Halogen Stress Corrosion Cracking of Zircaloy-4 Tubing", WAPD-TM-1149, July, 1974.

3. P. H. Kreyns, G. L. Spahr and J. E. McCauley, "An Analysis of Iodine Stress Corrosion Cracking of Zircaloy", WAPD-TM-1203, February, 1976.

4. R. P. Tucker, P. H. Kreyns and J. J. Kearns, "The Effects of Internal Surface Flaws, Iodine Concentration and Temperature on the Stress Corrosion Behavior of Zircaloy-4 Tubing", WAPD-TM-1248, February, 1976.

5. J. C. Wood, Interactions Between Stressed Zirconium Alloys and Iodine at 300°C", Nuclear Technology, 23, 63, (1974).

6. C. E. Ells and C. J. Simpson, "Stress Induced Movement of Hydrogen in Zirconium Alloys" in "Proc. of Conf. on Hydrogen in Metals", Seven Springs, Pa., September, 1973.

7. B. Cox and J. C. Wood, "Iodine Cracking of Zircaloy Fuel Cladding: A Review", Corrosion Problems in Energy Conversion and Generation, Craig S. Tedman, Jr. (ed.), Electrochemical Soc., New York, 1974.

8. B. Cox, "Environmentally Induced Cracking of Zirconium Alloys - A Review", Reviews in Coatings and Corrosion, 1, 367, (1975).

9. J. C. Wood, et al., "Environmentally Induced Fracture of Zircaloy by Iodine and Cesium", J. Nuclear Materials, 57, 155, (1975).

10. B. Cox, "Environmentally Induced Cracking of Zircaloy Alloys", Corrosion 28, 207, (1972).

11. D. Cubicciotti, et al., "EPRI-NASA Cooperative Project on Stress Corrosion Cracking of Zircaloys, Quarterly Progress Reports", Stanford Research Institute, Menlo Park, California., (a) November 15, 1975, (b) February 20, 1976, (c) May 21, 1976, (d) August 15, 1976, (e) November 12, 1976. A limited number of copies of these progress reports may be obtained from EPRI, Palo Alto, California.

12. W. T. Grubb, "Cadmium Metal Embrittlement of Zircaloy-2", Nature, 265, 36 (1977); W. T. Grubb and M. H. Morgan, III, "Cadmium Embrittlement of Zircaloy-2" to be published in "Proceedings, ANS Topical Meeting on Water Reactor Fuel Performance", St. Charles, Illinois, May, 1977.

13. J. Belle, Ed., Uranium Dioxide: Properties and Nuclear Applications (U.S.A.E.C., U. S. Government Printing Office, Washington, D. C. 1961) p. 478.

REFERENCES (Cont'd)

14. R. F. Boyle, GEAP-4452, 1964.

15. N. Fuhrman, et al., "Evaluation of Fuel Rod Performance in Main Yankee Core I", EPRI NP-218, Electric Power Research Institute, Palo Alto, California, November 1976.

16. J. T. A. Roberts, et al., "On the Pellet-Cladding Interaction Phenomenon," Nuclear Technology 35, 131, (1977).

TABLE I

Mechanical Properties of Zircaloy-4 Tubing Tested

Tubing Lot	Yield Strength* (psi)	Ultimate Tensile Strength (psi)	% Elongation (in 2 in.)	% Uniform Elongation	Contractile Strain Ratio $\frac{\epsilon_\theta}{\epsilon_r}\Big\|_{\sigma_\theta, \sigma_r = 0}$
		a. Room Temperature Data			
0-06 B,G	57030	83330	29.17	21.0	1.561
0-07 C	51200	78830	29.00	16.7	1.561
0-08 D	56330	82630	28.17	16.8	1.523
0-10 E	57630	89000	27.83	16.8	1.550
0-12 F,H	55430	80700	29.50	17.2	1.617
0-21 J	55200	80070	28.50	16.8	1.587
0-22 K	56730	81900	29.33	16.5	1.643
0-23 L	53800	78900	29.50	16.5	1.673
0-31 M	51200	77570	29.50	17.0	1.563
		b. 700°F Data			
0-06	18700	36630	36.83	22.8	
0-07	18600	36730	36.83	22.3	
0-08	19270	37100	36.00	22.7	
0-10	18470	35500	37.67	23.8	
0-12	18070	35730	37.67	23.7	
0-21	18730	36630	34.17	22.2	
0-22	18530	37030	34.17	22.2	
0-23	18670	36430	35.33	22.5	
0-31	18100	34300	38.17	23.8	

(Data are averages from three test samples per lot)

TABLE I (Cont'd)

c. Pressure Burst Data

Tubing Lot No.	Specimen No.	Test Temp. (°F)	Hoop Yield Strength (ksi)	Ultimate Hoop Tensile Stress (ksi)
0-06	B1	680	27.5	49.5
0-07	C3	680	28.6	47.5
0-08	D1	680	28.6	48.3
0-10	E3	680	26.4	44.1
0-12	F1	680	27.0	43.6
		Avg.	27.6	Avg. 46.6
0-06	B10	750	25.7	44.0
0-07	C10	750	27.3	43.8
0-08	D8	750	27.2	42.6
0-10	E8	750	25.8	41.4
0-12	F2	750	-	40.6
		Avg.	26.5	Avg. 42.5

* 0.2% strain offset

TABLE II

Internal Surface Flaw Characterization of RXA Zircaloy-4 Tubing

Tube No.	Specimen Prefix	Ave. Max. Flaw Depth (mils)	Maximum Flaw Depth (mils)	Flaw Geometry
0-06-02306	B	.15	.25	Random pits, some grooves
0-07-03145	C	.07	.18	Aligned elongated pits, some grooves
0-08-04167	D	.19	.22	Aligned grooves, some pits
0-10-06133	E	.31	.35	Pits and grooves
0-12-08500	F	.07	.18	Pits and grooves
0-06-02253	G	.15	.22	Pits, some small grooves
0-12-07886	H	.08	.13	Aligned elongated pits, some grooves
0-21-16415	J	.18	.19	Pits, some shallow grooves
0-22-17333	K	.17	.26	Rough-edged long grooves
0-23-17640	L	.18	.22	Pits, some elongated pits
0-31-24589	M	.07	.13	Grooves

TABLE III

Specimen Failure Data Illustrating the Effects of
Iodine SCC in Internally Pressurized RXA Zircaloy-4 Tubing

	Specimen	Test Temp. (°F)	Nominal σ_θ (ksi)	Nominal σ_θ At Failure Location ‡ (ksi)	Iodine mg/dm^2	Failure Time, HRS	Avg. Failure Time, HRS	Comments+
a.	D16*	750	40	40.0	4	1-2	1.5	
	D7 *	750	40	39.1	0.5	3-4	3.5	
	E15*	750	40	40.0	0.1	20.5	20.5	Ruptured
	D12*	750	40	40.0	0.1	23-24	23.5	Slight bow, bulge
	D10	750	40	40.0	0	61.25	61.25	Ruptured
	D13*	750	35	35.0	4	3-4	3.5	
	D5 *	750	35	35.0	4	3-4	3.5	
	D18*	750	35	35.0	0.5	17-18	17.5	
	D15	750	35	35.0	0.1	18-19	18.5	Badly bowed, bulged
	D21	750	35	35.0	0.1	176-184	180	Badly bowed, bulged
	D20*	750	30	29.6	4	7-8	7.5	
	D17*	750	30	29.7	0.5	60-64	62	Slight bow
	D3 *	750	30	29.3	0.1	252-259	255.5	
	D14	750	30	30.0	0	95-101	98	Badly bowed
	D19*	750	22	22.0	4	48-50	49	
	D9	750	22	22.0	0.1	1468-1515	1492	Bowed, bulged
b.	E11*	720	35	35.0	4	4-5	4.5	Slight bow
	E7 *	720	35	31.6	0.5	120-123	121.5	Slight bow
	E6 *	720	35	33.2	0.1	208-216	212	Slight bow
	E9	720	35	35.0	0	408-424	416	Bowed, slight bulge

TABLE III (Cont'd)

	Specimen	Test Temp. (°F)	Nominal σ_θ (ksi)	Nominal σ_θ At Failure Location ‡ (ksi)	Iodine mg/dm²	Failure Time, HRS	Avg. Failure Time, HRS	Comments+
	E19*	720	30	30.0	4	24-25	24.5	
	E4 *	720	30	29.2	4	26-27	26.5	
	E10	720	30	30.0	0.5	12-13	12.5	Slight bow, large wall eccentricity
	E17	720	30	30.0	0.1	1740-1787	1764	Bowed, bulged
	E13	720	30	-	0.1	-	-	> 4773 hrs.
	E18	720	30	-	0	2061-2163	2112	Bowed, bulged
	E20*	720	25	24.8	4	48-50	49	
	E14	720	25	-	0.1	-	-	> 4773 hrs.
	E16	720	25	-	0	-	-	> 4773 hrs.
c.	E12	680	40	36.9	4	.75	.75	Ruptured, bowed
	F19	680	40	38.9	4	7-8	7.5	Bowed
	F12	680	40	39.7	0.5	15-16	15.5	Bowed, split
	F20	680	40	40.0	0.1	88-91	89.5	Badly bowed, bulged
	F13	680	40	37.0	0	119-125	122	Badly bowed, bulged
	F5 *	680	35	35.0	4	75-79	77	
	F7 *	680	35	35.0	0.5	124-130	127	
	F4 *	680	35	34.7	0.1	2338-2386	2362	Slight bow, uniformly bulged
	F8	680	35	34.4	0	2001-2072	2036.5	Badly bowed, bulged
	F16*	680	30	29.7	4	124-130	127	
	F10	680	30	29.9	4	16-17	16.5	Bowed, wall eccentricity not measured
	F17*	680	30	33.0‡‡	0.5	154.5-159.5	157	
	F15	680	30	-	0.1	-	-	> 8054 hrs.
	F11*	680	30	29.3	0.1	3146-3217	3182	Slight bow, slight bulge
	F18	680	30	30.0	0	-	-	> 8054 hrs.

TABLE III (Cont'd)

	Specimen	Test Temp. (°F)	Nominal σ_θ (ksi)	Nominal σ_θ At Failure Location ‡ (ksi)	Iodine mg/dm^2	Failure Time, HRS	Avg. Failure Time, HRS	Comments[+]
	F14	680	25	27.5‡‡	4	88-91	89.5	Bowed, eccentric wall
	F9	680	25	-	0.1	-	-	> 4542 hrs.
d.	B6 *	680	40	40.0	4	11-12	11.5	
	B9 *	680	40	40.0	0.5	64-66	65	Slight bulge
	B21	680	40	40.0	0.1	88-91	89.5	Badly bowed, bulged
	B16	680	40	40.0	0	199	199	Ruptured, badly bowed, bulged
	B3 *	680	35	35.0	4	17-18	17.5	
	B18	680	35	35.0	0.5	23-24	23.5	Bowed
	B12	680	35	35.0	0.1	1159-1246	1203	Badly bowed, slight bulge
	B19	680	35	35.0	0	795-818	807	Badly bowed, bulged
	B20*	680	30	29.0	4	44-46	45	
	B2 *	680	30	30.0	4	70-74	72	
	B15	680	30	30.0	0.5	2737-2784	2761	Bulged
	B14	680	30	-	0.1	-	-	> 4542 hrs.
	B5	680	30	-	0.1	-	-	> 4542 hrs.
	B7	680	30	-	0	-	-	> 4542 hrs.
e.	K6	680	40	38.8	4	8-9	8.5	
	K16	680	40	-	0.1	-	-	> 577 hrs.
	K9	680	35	32.9	4	25-27	26	
	K17	680	35	-	0.5	83-90	86.5	Weld failure
	K15	680	35	-	0.1	-	-	> 577 hrs.
	K14	680	35	-	0	-	-	> 577 hrs.
	K10	680	30	27.5	4	48-52	50	
	K12	680	30	-	0.5	-	-	> 577 hrs.
	K13	680	30	-	0.1	-	-	> 577 hrs.

TABLE III (Cont'd)

	Specimen	Test Temp. (°F)	Nominal σ_θ (ksi)	Nominal σ_θ At Failure Location ‡ (ksi)	Iodine mg/dm^2	Failure Time, HRS	Avg. Failure Time, HRS	Comments+
	K22	680	30	-	0	-	-	> 577 hrs.
	K11	680	25	23.9	4	211-227	219	
f.	H8 *	680	40	37.0	0.5	594-664	629	
	H1	680	40	-	0.1	-	-	> 1438 hrs.
	H13	680	40	-	0	-	-	> 1438 hrs.
	H7	680	35	-	0.5	-	-	> 1438 hrs.
	H17	680	35	-	0.1	-	-	> 1438 hrs.
	H12	680	35	-	0	-	-	> 1438 hrs.
	H6	680	30	-	0.5	-	-	> 1438 hrs.
	H16	680	30	-	0.5	-	-	> 1438 hrs.
	H20	680	30	-	0.1	-	-	> 1438 hrs.
	H5	680	30	-	0	-	-	> 1438 hrs.
	H15*	680	25	25.3	4	548-594	571	
g.	G6	680	30	29.3	4	59-62	60.5	
	G9	680	25	24.4	4	118-126	122	
h.	J6	680	30	30.2	4	48-52	50	
	J9	680	25	23.3	4	635-706	671	

‡ Stress calculated using the pre-test I.D. and O.D. at the actual failure location unless otherwise noted.

‡‡ Stress based on post-test measurement of tube wall eccentricity at the failure site.

\+ Unless noted, specimens are straight and not bulged.

* These specimens appear in Figure 2 and are the data base for evaluating the stress corrosion sensitivity to iodine concentration.

TABLE IV

Specimen Failure Data Illustrating the Effects of Iodine SCC in Internally Pressurized RXA Zircaloy-4 Tubing at 720°F Near Threshold

Specimen	Nominal σ_θ (ksi)	Nominal σ_θ at Failure Location (ksi)	Iodine Concentration (mg/dm^2)	Failure Time (hr.)	Time in Test (Specimens Surviving) (hr.)
B17	35	-	0.1		> 1649
C4	35	36.6	0.1	783-853	
C18	35	-	0.1		> 1649
G18	35	-	0.1		> 1649
G20	35	35.0	0.1	305-312	
G10	35	-	0.1		> 767
H2	35	-	0.1		> 1649
H19	35	35.0	0.1	906 (rupture)	
J17	35	-	0.1		> 1649
J20	35	33.2	0.1	260-282	
J18	35	-	0.1		> 767
K20	35	33.2	0.1	409-432	
K23	35	32.8	0.1	138-162	
K21	35	-	0.1		> 767
L5	35	-	0.1		> 1649
B13	30	-	0.1		> 1649
B8	30	-	0.1		> 1649
C6	30	-	0.1		> 1649
C21	30	-	0.1		> 1649
G14B	30	-	0.1	1460-1554	
G16	30	-	0.1		> 1649
G12	30	-	0.1		> 767
H4	30	-	0.1		> 1649
H18	30	-	0.1		> 1649
J15	30	-	0.1		> 1649
J19	30	-	0.1		> 1649
J23	30	-	0.1		> 767
K18	30	-	0.1		> 1649
K19	30	-	0.1		> 1649
K24	30	-	0.1		> 767
L3	30	-	0.1		> 1649

TABLE V

Calibration Data for Iodine SCC Threshold Stress Temperature Dependence in RXA Zircaloy-4 Tubing

Tubing Lot	σ_{th} (ksi)	T (°F)	I_2 Conc. (mg/dm^2)	a_o (in.)	Y
J	23.0	680	4	.0002	2.0
D	21.0	750	4	.0002	2.0
Reference 2 data	23.0	680	4	.0002	2.0
	21.0	750	4	.0002	2.0

TABLE VI

Calculated I_2 SCC Threshold Stresses as a Function of I_2 Concentration and Temperature for a Typical Flaw (a_o = 0.00025), Y = 2.0

I_2 Conc. (mg/dm^2)	T (°F) 680 (ksi)	720 (ksi)	750 (ksi)
4	20.6	19.6	18.8
0.5	30.9	29.3	28.2
0.1	42.2	40.2	38.5

TABLE VII

Effect of Water Vapor on Iodine SCC in RXA Zircaloy-4 Tubing

Spec. No.	I_2 Conc. (mg/dm^2)	H_2O Conc. (ppm)	T (^oF)	Nominal σ_θ (ksi)	Initial σ_θ at Failure Location (ksi) *	Initial σ_θ at Failure Location (ksi) **	Failure Time (hr.)
M7	4	~ 2	680	35	33.9	35.6	14-15
M16	4	~ 2	680	25	23.0	23.5	215-238
M9	4	~ 2	750	35	34.6		2-3
M19	4	~ 2	750	25	23.9		25-33
M20	0.1	~ 2	680	30	-		> 2159 (in test)
M15	4	< .03	680	35	32.6	30.0	16-17
M12	4	< .03	680	25	23.4	23.5	736-834
M17	4	< .03	750	35	33.2		2-3
M18	4	< .03	750	25	±		86-109
M10	0.1	~ .05	680	30	-		> 2159 (in test)
M8	4	~ 2	680	25	22.7		271-343
M6	4	<.03	680	25	22.1		271-343

*Stress calculated using the pre-test I.D. and O.D. at the actual failure location.
**Best estimate stress, based on post-test measurement of tube wall eccentricity at the failure site.
± Failure in specimen shoulder outside gage length.

TABLE VIII

Effects of Tubing Hydrogen Content on
Iodine SCC in Internally Pressurized RXA Zircaloy-4 Tubing

Specimen No.	H Conc.‡ (ppm)	I_2 Conc. (mg/dm^2)	T (°F)	Nominal σ_θ (ksi)	Estimated Nominal σ_θ at Failure Location (ksi)		Failure Time (hr.)
					*	**	
L6	20	0	680	35	-	-	> 2266 (in test)
L14	190	0	680	35	-	-	> 2266 (in test)
L7	20	4	680	35	32.0	32.1	102-119
L10	60	4	680	35	33.0	33.5	45-50
L12	60	4	680	35	33.9	34.5	68-75
L15	190	4	680	35	35.0	35.5	34-42
L19	190	4	680	35	34.5	34.9	97-105
L8	20	0	600	40	-	-	> 1942 (in test)
L16	190	0	600	40	-	-	> 1942 (in test)
L9	20	4	600	40	36.2	36.2	967-1013
L11	60	4	600	40	38.6	38.9	347-371
L17	190	4	600	40	38.6	38.9	371-394

‡ Analytical chemistry H analyses of representative specimens.
* Stress Calculated using the pre-test I.D. and O.D. at the actual failure location.
** Best estimate stress based on post-test measurement of tube wall eccentricity at the failure site.

TABLE IX

Internally Pressurized RXA Zircaloy-4
Tubing Cesium Stress Corrosion Tests

Specimen No.	Cs Conc. (mg/dm^2)	I_2 Conc (mg/dm^2)	T (^oF)	Nominal σ_θ (ksi)	Test Time (hr.)
M5	28	0	680	35	> 2610
M11	28	0	680	35	> 2610
M2	800	0	680	35	> 1886
M13	28	0	750	35	729-760 (failed by stress rupture)
M1	28	4	680	30	> 1886
M4	28	4	680	30	> 1886
M14	28	0	392	35	> 2856
M3	3200	0	392	35	> 2130

TABLE X

Internal Mandrel Strain-Controlled Iodine SCC Test Parameters for RXA Zircaloy-4 Tubing Specimens

Specimen No.	I_2 Concentration (mg/dm^2)	Initially Applied Total Hoop Strain (%)	Test Temp. (^oF)	Test Duration (Hrs.)
G7	4	0.34	680	77
J1	4	0.34	680	77
K1	4	0.34	680	77
G2	4	0.34	680	2015
J2	4	0.34	680	2015
K2	4	0.34	680	1007
G4	50	0.34	680	77
J4	50	0.34	680	77
K8	50	0.34	680	77
G5	50	0.34	680	2015
J8	50	0.34	680	2015
K5	50	0.34	680	1007
J7	50	0.29	600	2015
K7	50	0.29	600	72

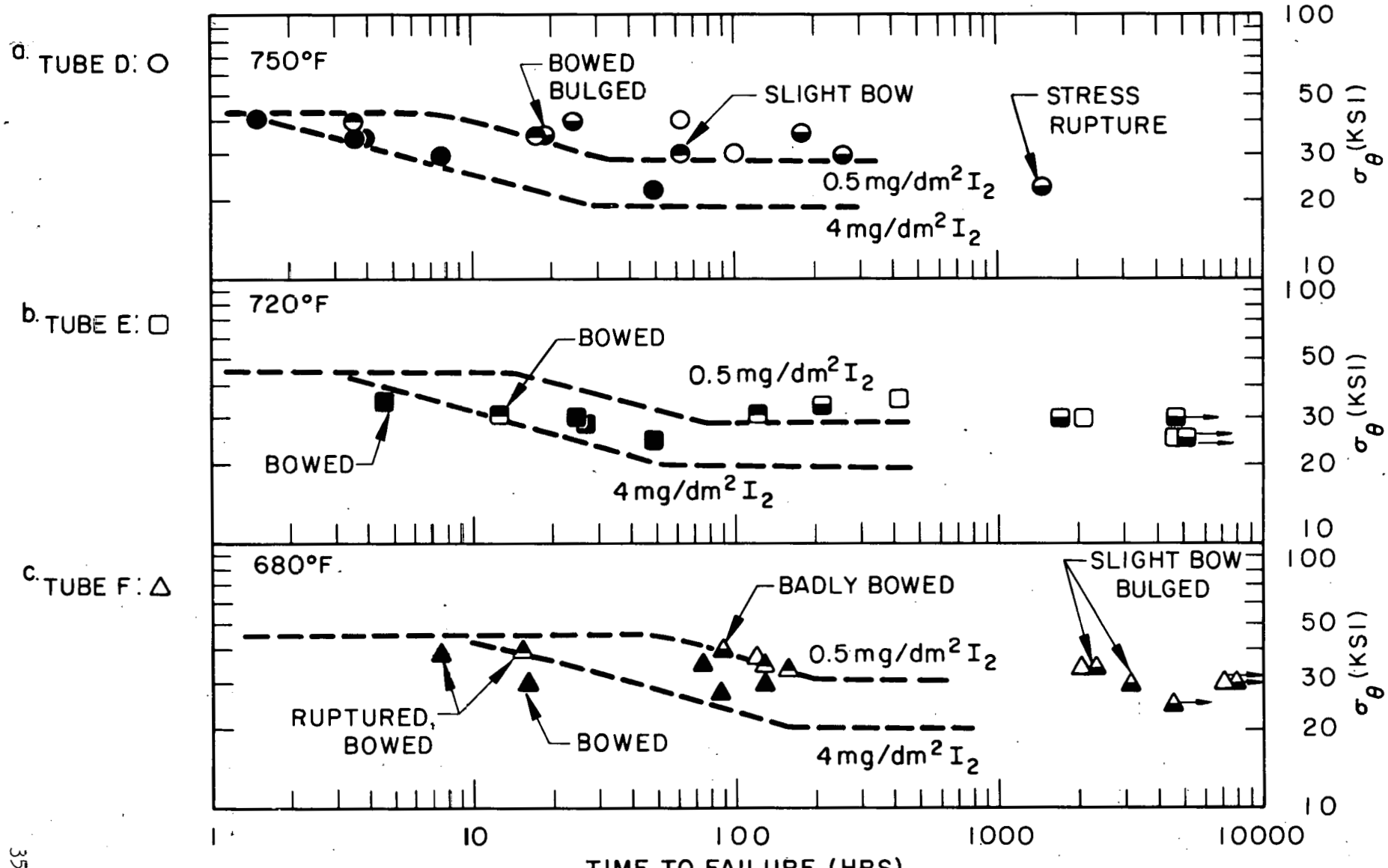

FIGURE 1 - Time to Failure Data of Table III. (Fully shaded symbols: 4 mg/dm^2 I_2; upper-half shaded: 0.5 mg/dm^2 I_2; lower half shaded: 0.1 mg/dm^2 I_2; open symbols: 0 mg/dm^2 I_2). Curves are the predictions of Equations (5) and (7), for Y = 2 and a_o = 0.00025 in.

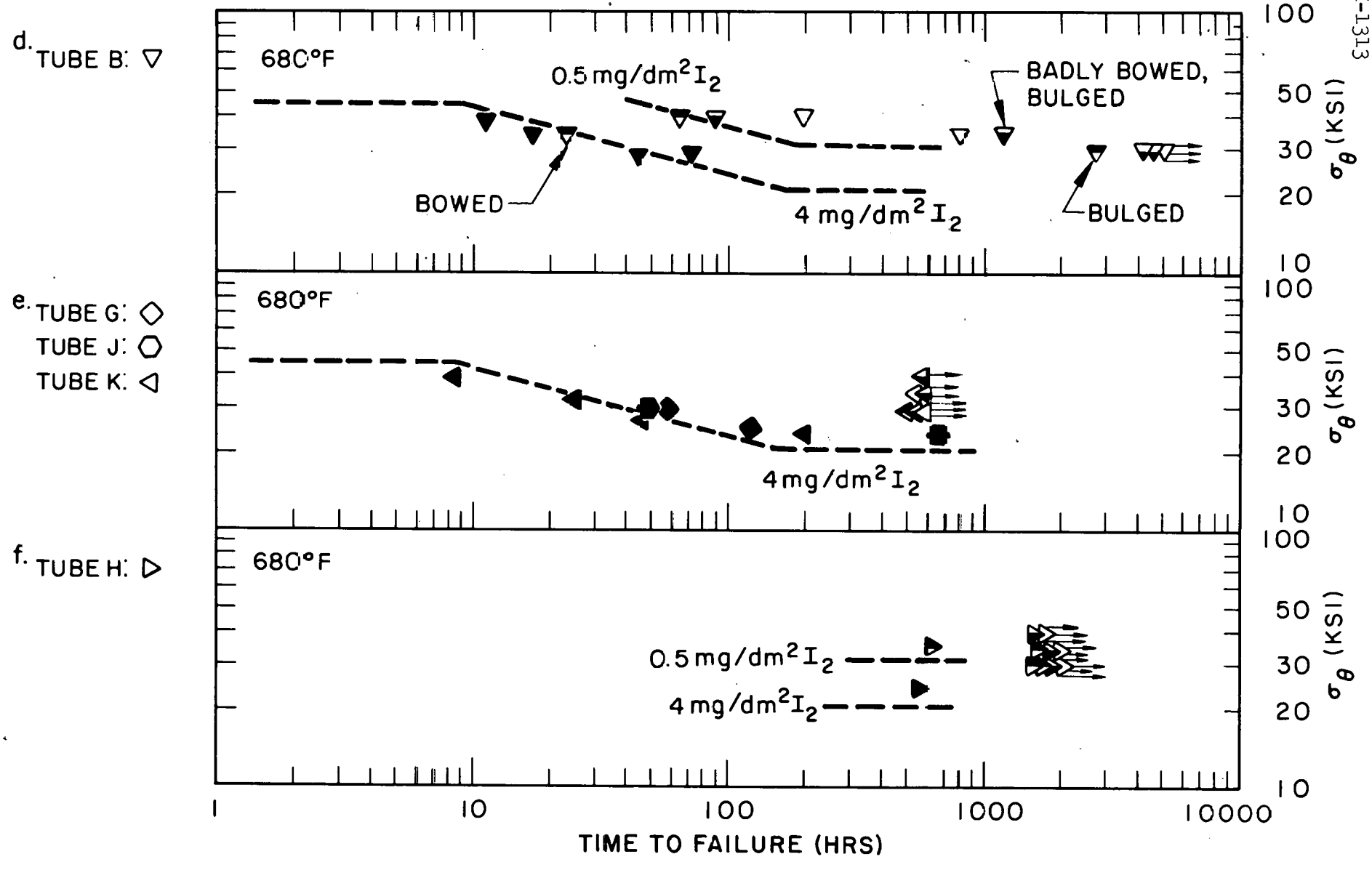

FIGURE 1 (Cont'd)

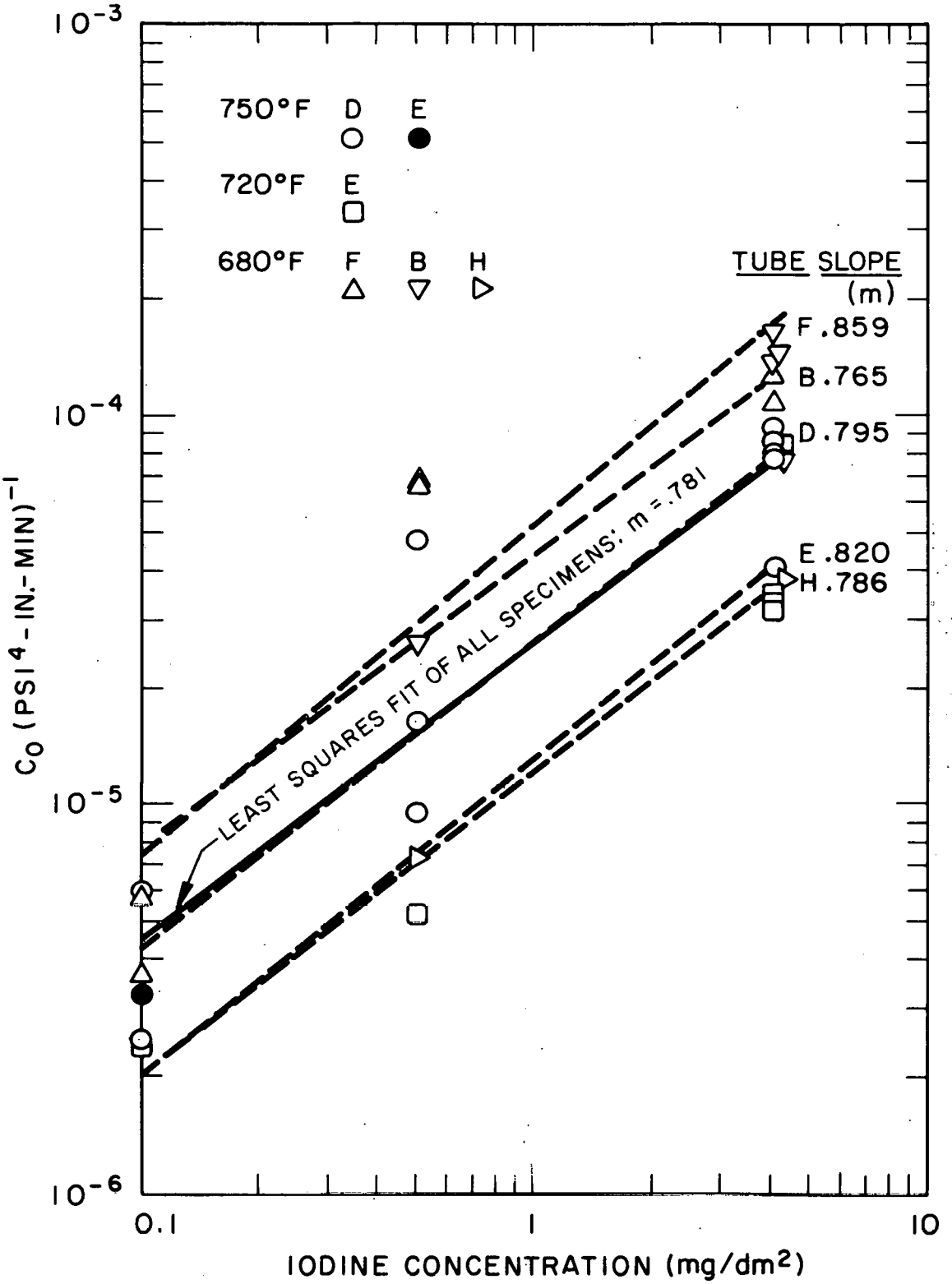

FIGURE 2 - Iodine Sensitivity of SCC in RXA Zircaloy-4 Tubing. (Letters assigned to symbols identify the particular tubing length).

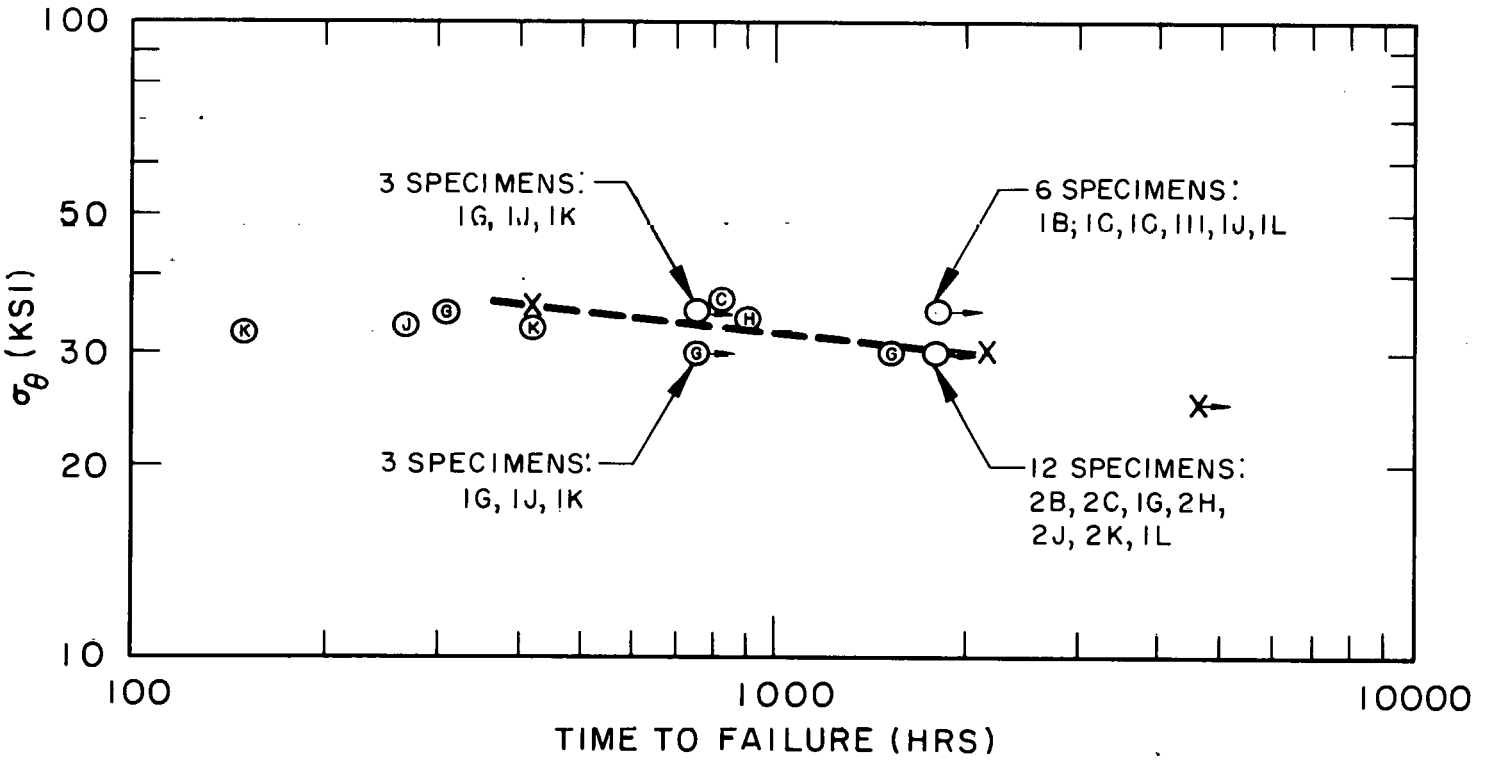

FIGURE 3 - Iodine SCC Threshold Stress Test Data at 720°F, 0.1 mg/dm^2 I_2. Initial Hoop Stress as a Function of Time to Failure. (Specimens containing no I_2 which failed by stress rupture are indicated by X and the broken line. Letters assigned to symbols identify the particular tubing length).

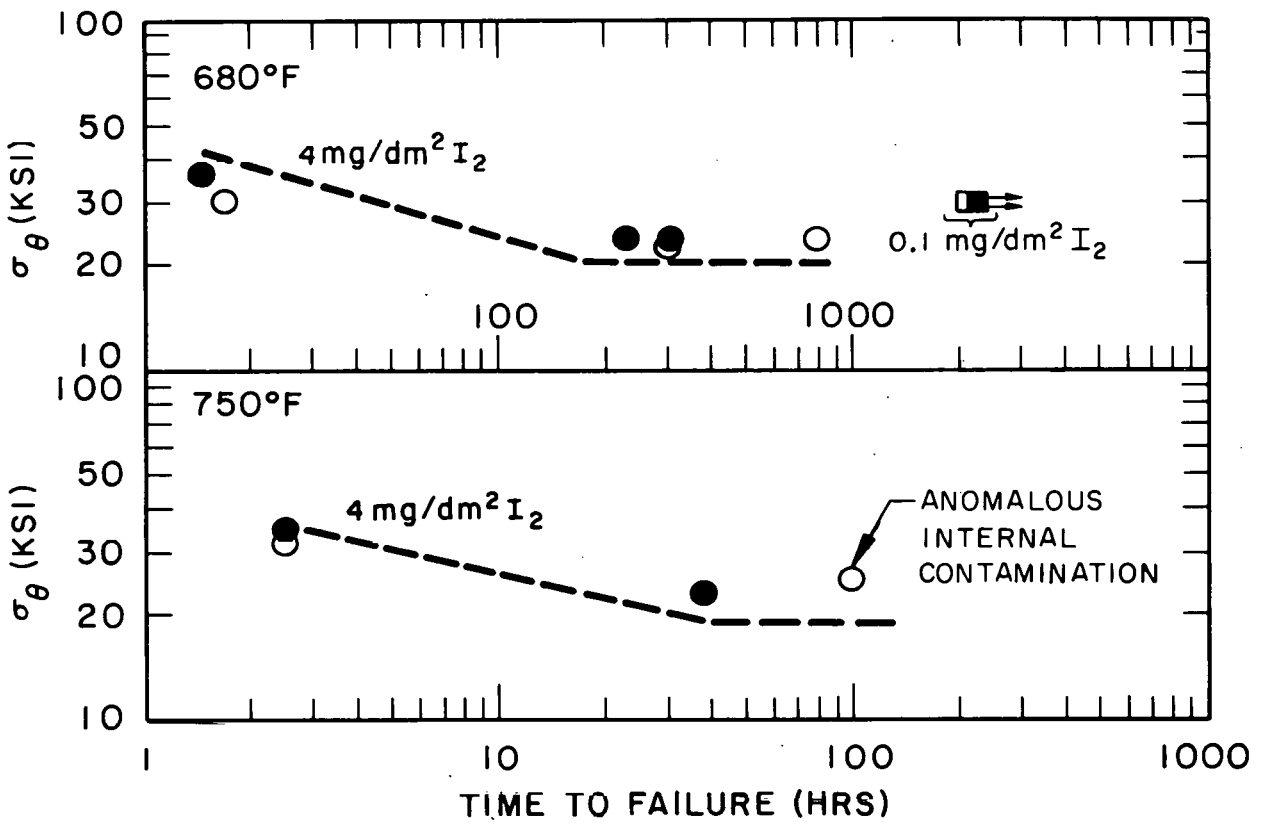

FIGURE 4 - Effect of Water Vapor on Iodine SCC in RXA Zircaloy-4 Tubing. (Shaded symbols are nominal H_2O, open symbols are low H_2O. All specimens contain 4 mg/dm² I_2 except as indicated). The calculated 4 mg/dm² I_2 curves for Y = 2 and a_o = 0.00025 in. are also shown.

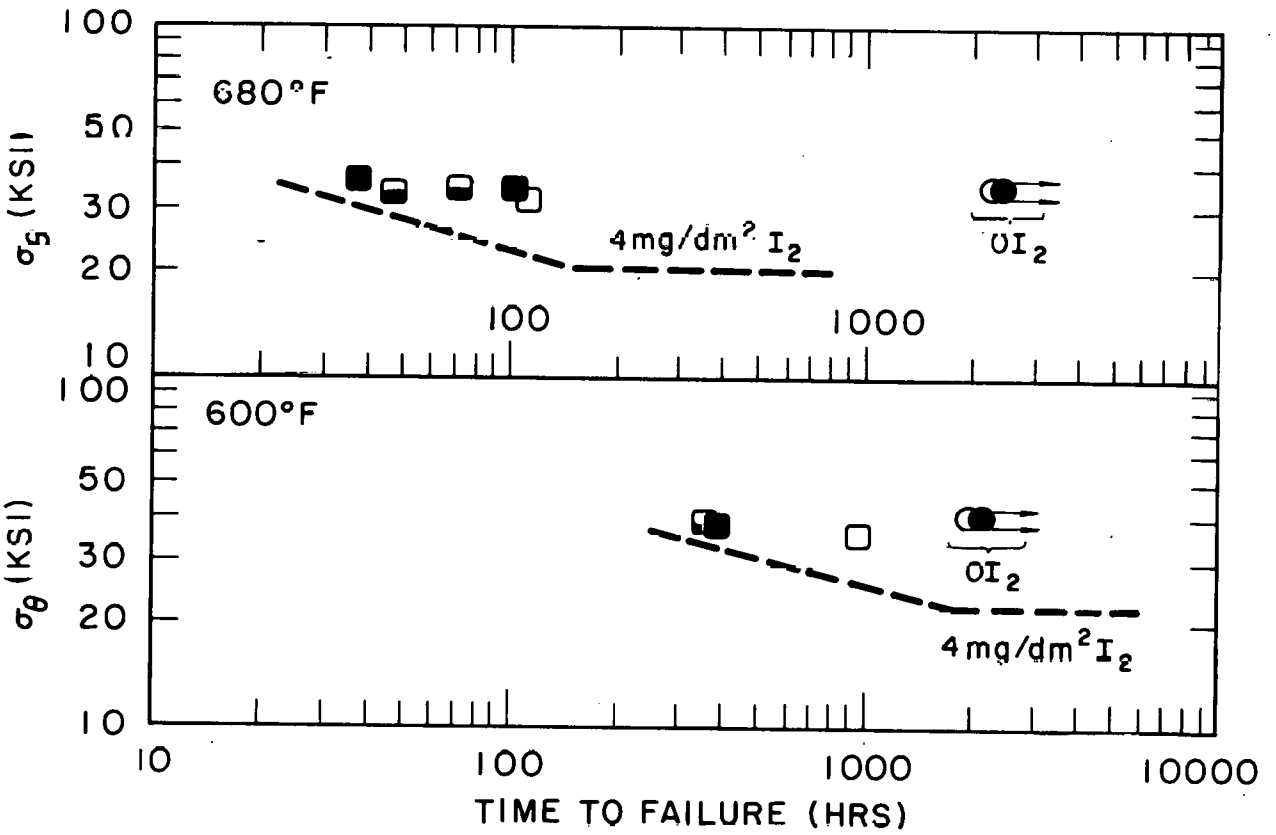

FIGURE 5 - Effect of Tubing Hydrogen Content on Iodine SCC in RXA Zircaloy-4 Tubing. (Shaded symbols are 100 ppm H; half-shaded symbols are 60 ppm H; open symbols are 20 ppm H. All specimens contain 4 mg/dm^2 I_2 except as indicated. The calculated 4 mg/dm^2 I_2 curves, for Y = 2 and a_o = 0.00025 in. are also shown.

*U.S. GOVERNMENT PRINTING OFFICE: 1977-703-115/71